Earthq Eng & Eng Vib (2015) 14: 315-328 **DOI**:10.1007/s11803-015-0025-2

Optimization for performance-based design under seismic demands, including social costs

Oscar Möller[1†], Ricardo O. Foschi[2†], Juan P. Ascheri[1†], Marcelo Rubinstein[1†] and Sergio Grossman[1†]

1. *Instituto de Mecánica Aplicada y Estructuras* (*IMAE*), *Facultad Cs.Ex., Ingenieríay Agrimensura, Universidad Nacional de Rosario, Riobambay Berutti, 2000 Rosario, Argentina*

2. *Civil Engineering Department, University of British Columbia, 6250 Applied Sciences Lane, Vancouver, B.C., Canada V6T 1Z4*

Abstract: Performance-based design in earthquake engineering is a structural optimization problem that has, as the objective, the determination of design parameters for the minimization of total costs, while at the same time satisfying minimum reliability levels for the specified performance criteria. Total costs include those for construction and structural damage repairs, those associated with non-structural components and the social costs of economic losses, injuries and fatalities. This paper presents a general framework to approach this problem, using a numerical optimization strategy and incorporating the use of neural networks for the evaluation of dynamic responses and the reliability levels achieved for a given set of design parameters. The strategy is applied to an example of a three-story office building. The results show the importance of considering the social costs, and the optimum failure probabilities when minimum reliability constraints are not taken into account.

Keywords: earthquake engineering; performance-based design; optimization; reliability; social costs

1 Introduction

Performance-based design is a general approach by means of which a structure is designed to meet with confidence specified performance criteria for different limit states. Its application to earthquake engineering has been the subject of many previous studies (Bertero, 1997; Ghobarah, 2001; Hamburger *et al*., 2004), and forms the basis for modern Code specifications. These studies have highlighted the role played by the uncertainties present in both the structural performance as well as in the ground motions.

In this work, performance-based design in earthquake engineering is defined as the determination of design parameters by means of an optimization process, the aim of which is the minimization of an objective function incorporating the total cost of the structure, while satisfying minimum target reliabilities for the specified performance criteria and limit states.

Using a different approach to that from previous works, this paper does not use fragility data and integration over earthquake intensity demands (Hamburger *et al*., 2004). Fragilities represent the structural global response to a specified demand, and include the effect of underlying design variables like structural dimensions, steel reinforcements, etc. Each change in structural parameters will demand a re-calculation of the fragilities and this, in turn, will not be efficient for structural optimization. In the present paper, we study the structural responses directly as functions of all the intervening variables, including the characteristics of ground motions and design parameters like dimensions and amount of reinforcement. This allows representation of the structural responses by means of continuous response surfaces. These, in turn, facilitate computer simulation for reliabilities achieved as the design is modified during the optimization to minimize the total cost.

The total costs normally include construction costs as well as those for repair of damage occurring during the economic life of the structure. In this paper, expanding the previous work presented in Möller *et al*. (2009a), we also incorporate in the objective the initial and damage-related costs associated with non-structural elements and building contents. Furthermore, we include the social costs associated with injuries and fatalities, loss of economic activity and stocks, and cost of temporary facilities, as these costs are directly related to the risks and characteristics of the structure being optimized.

The optimization must take into account all the uncertainties present. These stem from the ground

Correspondence to: Ricardo O. Foschi, Civil Engineering Department, University of British Columbia, 6250 Applied Sciences Lane, Vancouver, B.C., Canada V6T 1Z4
Tel: +1 604 822 2560
E-mail: rowfa1@civil.ubc.ca
†Professor

Received March 26, 2014; **Accepted** December 11, 2014

motion as well as from the random properties in the behavior of the structural components. In the context of performance-based design (SEAOC Vision 2000, 1995; FEMA 356, 2000) minimum target reliability levels (or acceptable levels of annual failure probabilities) are specified for the different performance levels considered: either for operational limits, or for life safety or at total collapse.

The performance requirements are formulated in terms of maximum structural responses during the earthquake. These maxima are obtained through nonlinear dynamic analyses for specific combinations of the random variables in the problem. It is efficient to represent these discrete results with continuous (response surface) functions, which can then be used as substitutes for the dynamic analysis (Hurtado, 2004). Different polynomial forms for response surfaces have been considered, but those based on neural networks have been found to offer advantages of flexibility and adaptability (Möller *et al*., 2009b) and they are used in this work. Any type of response surface, when adequately adjusted, offers computational efficiency when estimating failure probabilities through simulation procedures (Melchers, 1987).

The problem is restricted to size optimization, maintaining fixed the layout of the structural system. The process must consider constraints in probabilistic terms, the dimensionality of the problem, the form and the number of the different objective functions. The optimization algorithms can implement different strategies (Pérez López, 2005; Swisher *et al*., 2000; Gencturk and Elnashai, 2012), some requiring the calculation of gradients within schemes of steepest descent or of conjugate gradients (Bertero *et al*., 1979; Pezeshk, 1998). Other strategies are not gradient-dependent, and utilize heuristic schemes like random search or genetic algorithms (Liu *et al*., 2006; Fragiadakis *et al*., 2006; Lagaros and Papadrakakis, 2007). In this work we utilize a random search algorithm which has been developed previously by the authors (Möller *et al*., 2010, 2012a, 2012b). Starting from an initial design point, the optimization parameters are randomly perturbed within a search zone. The parameters corresponding to the least cost, satisfying the minimum reliability constraints, are then taken as the new initial or anchorage point, initiating a subsequent cycle in the random search. This iteration is continued until no parameter combination, within the search zone, is found to lead to a cost lower than that corresponding to the anchorage. This optimum combination is further validated by increasing the size of the search zone and repeating the scheme.

Apart from the introduction here of specific earthquake performance criteria and their associated target minimum reliability levels, the problem can also be classified as a Life Cycle Cost analysis (LCC), as shown in examples from the relevant literature (Gencturk, 2012).

The optimization methodology proposed here, although general, is described in the context of the example shown in the following section: a three-story reinforced concrete frame for an office building in the city of Mendoza, a high-seismic risk region of Argentina.

2 The structural system

The structure to be optimized is a three-story office building with spans and columns as shown in Fig. 1, both in plan and for a portal along the *x*-direction, which is the assumed direction of the earthquake motion.

Figure 1 shows the floor slabs, uniformly loaded with a load q; the column and beam dimensions in centimeters (cm); the longitudinal reinforcement A_{sc} and reinforcement ratio ρ_c for the columns; and those corresponding to the beams, A_{sb} and ρ_b for reinforcement at the bottom (midspan) and A'_{sb} and ρ'_{sb} at the supports.

3 The optimization process for performance based design

Figure 2 shows the organization of the optimization process. It is divided into blocks that can be executed separately but in sequence.

4 Block 1: structural analysis

4.1 Variables

Table 1 shows the variables $X(1)$ to $X(11)$, components of $\boldsymbol{X}$, which are included in the dynamic structural analysis to obtain a set of discrete responses. This table also shows the lower and upper bounds for the variables, within which combinations for analysis are chosen via experimental design. Bounds for variables

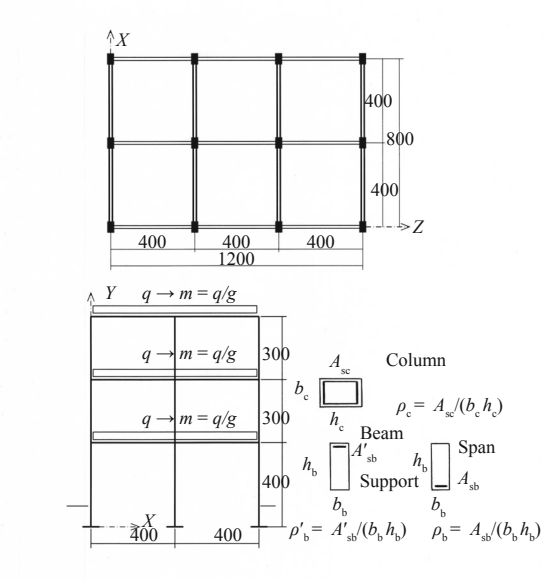

Fig. 1 Structural system

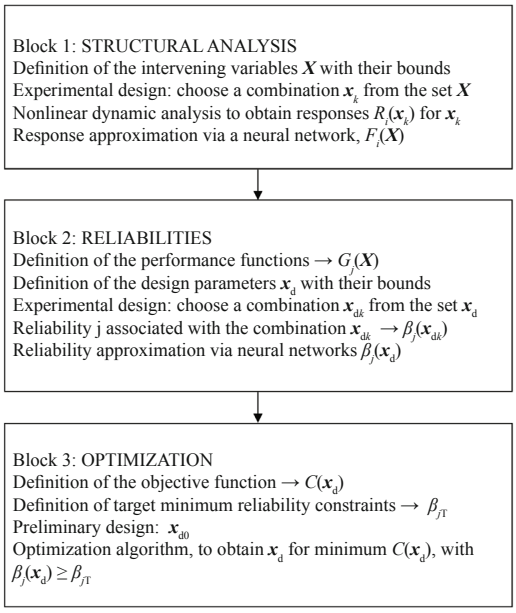

Fig. 2 Block organization for the optimization process

corresponding to reinforcement ratios must implement design Code requirements. Furthermore, Eqs. (1) and (2) show additional relationships to be satisfied. For example, Eq. (2) is to be satisfied to achieve a minimum, code-required beam strength under just gravitational loads.

$$0.5\,\rho'_s \leq \rho_s \leq 2\,\rho'_s \tag{1}$$

$$\rho'_s + \rho_s \geq \frac{1.40\,q\,l^2}{6.48\,b_b\,h_b^2\,f_y} \tag{2}$$

The design procedure specified in the Code for Argentina (INPRES-CIRSOC 103, 2008), Part I, is based on a demand combination of permanent (D), live (L) and earthquake (E) loads: $1.0\,D + 0.25\,L \pm E$. For the structure in Fig. 1, and assuming a permanent load D = 6.80 kN/m^2 and a live load L = 2.5 kN/m^2, a total load W = 712.8 kN is obtained per story. Since the floor slabs are assumed to be rigid diaphragms, each portal must resist 1/4 of the total seismic demand. Thus, a mean value for the mass applied to the beams, per unit length, can be calculated to be $m = 2.27\ 10^{-4}$ kN s^2 / cm^2.

The seismic action E corresponds to the specified ground motions. These have to be selected to constitute a set of records likely to occur at the site. Of course, this is not a simple task, and several techniques are normally used to produce such a set, including the use of historical records (when available). Here, ground accelerograms are artificially generated (Shinozuka and Sato, 1967; Möller, 2001) following a procedure for which two basic variables are required: the peak ground acceleration a_G at the site and the central frequency for the ground filter, f_g. Following Shinozuka, a Normal random phase angle is introduced with each of the frequencies and a modulation function is applied to introduce non-stationarity. Other methods can be similarly used for the specific characterization of the ground motions, as the approach chosen does not affect the optimization procedure described in this work.

4.2 Variable combinations

Design of experiments was applied to generate, randomly, NP = 450 combinations of the intervening variables. The range of $X(10)$ between its corresponding bounds was divided into three sectors, while only one sector was used between the bounds of each of the remaining variables. Each combination was then obtained by choosing a random value for a variable within each corresponding sector. The process was repeated 150 times, resulting in a total of NP = 450 variable combinations. This number permits 1) an adequate coverage of the variable ranges, and 2) that the neural network which will be used to approximate

Table 1 Variables and their bounds

Variable	Lower bound	Upper bound	Definition
$X(1) = m$ (kN·s^2 / cm^2)	1.50×10^{-4}	3.00×10^{-4}	Beam mass per unit length
$X(2) = b_b$ (cm)	15	30	Beam section width
$X(3) = h_b$ (cm)	30	70	Beam section depth
$X(4) = b_c$ (cm)	20	40	Column section width
$X(5) = h_c$ (cm)	30	100	Column section depth
$X(6) = \rho_b$	0.00298	0.01389	Beam reinforcement ratio (midspan)
$X(7) = \rho'_b$	0.00298	0.01389	Beam reinforcement ratio (supports)
$X(8) = \rho_c$	0.008	0.04286	Column reinforcement ratio
$X(9) = f_r/f'_{c0}$	0	0.15	Confinement pressure (normalized)
$X(10) = a_G$ (cm / s^2)	10	1200	Peak ground acceleration
$X(11) = f_g$ (Hz)	1.50	3.50	Central ground filter frequency

the corresponding dynamic responses could have an architecture with a maximum of 25 neurons in one hidden layer, in order to achieve satisfactory precision in the predictions (Möller *et al*., 2010).

For each of the 450 combinations of the variables in Table 1, a set of NS = 10 sub-combinations were obtained. Each of these correspond to: 1) a different random choice for the phase angle associated with each frequency in the generation of an artificial accelerogram, that is, a *different ground motion*, and 2) a different concrete strength and steel yield point, parameters that directly affect the moment-curvature relation for the beams and columns (Möller *et al*., 2006).

4.3 Nonlinear dynamic analysis

A nonlinear dynamic analysis is performed for each combination of the variables and for each of the corresponding sub-combinations. The background for the structural model used in this analysis is described elsewhere (Möller, 2001; Möller *et al*., 2006; Möller and Foschi, 2003) and is similar to that proposed by Filippou *et al*. (1992).

The maximum responses, which enter into the different performance functions, are then obtained: UMAX: maximum horizontal displacement at the top of the structure; AMAX1: maximum acceleration for the first story; AMAX2: maximum acceleration for the second story; DISTM: maximum inter-story drift; DIES: global damage index; DILOM: maximum local damage index. This work uses damage indices as defined by Park and Ang (1985) and Möller *et al*. (2009a).

If R is a generic response, the corresponding calculated responses $R_{k,j}$ are obtained for each combination j = 1, NP and each sub-combination k = 1, NS. For each of the NP combinations, the results are then used to calculate the mean response and the standard deviation over the set of NS sub-combinations:

$$\overline{R}_j = \frac{1}{\mathrm{NS}} \sum_{k=1}^{\mathrm{NS}} R_{k_j}\,;\ \sigma_{R_j} = \sqrt{\frac{1}{\mathrm{NS}-1} \sum_{k=1}^{\mathrm{NS}} (R_{k_j} - \overline{R}_j)^2} \tag{3}$$

4.4 Neural network approximations for the responses

The NP results from Eq. (3) are used to train two neural networks (Möller *et al*., 2009b), one for the mean value and another for the standard deviation of the responses over the set of sub-combinations. The implementation of the network has the general form

$$R(\boldsymbol{X}) \cong F(\boldsymbol{X}) = h\,(\sum_{j=1}^{J} W_{kj}\ h(\sum_{i=1}^{N} W_{ji}\ X_i + W_{j0}) + W_{k0}\,) \tag{4}$$

in which $R(\boldsymbol{X})$ is the value obtained for the particular combination of the variables $\boldsymbol{X}$, $F(\boldsymbol{X})$ is the neural network approximation, W_{kj} and W_{ji} are weight factors to be calculated during network training, and $h(t)$ is a nonlinear transfer function. Details on $h(t)$ used and the calculation of the weight factors can be found in previous publications by the authors (Möller *et al*., 2009a, 2012b). The training implies the optimization of the weights W so that the differences between the network predictions and the dynamic analysis results are minimized.

Since the training or the approximation of $R(\boldsymbol{X})$ with $F(\boldsymbol{X})$ is normally very good but never perfect (see, for example, Fig. 3 for DISTM), there is a scattering around the network predictions that can be quantified with the standard deviation of the relative error:

$$\sigma_{\varepsilon_r} = \sqrt{\frac{1}{\mathrm{NP}-1} \sum_{k=1}^{\mathrm{NP}} (\frac{Y_k - T_k}{Y_k})^2} \tag{5}$$

in which Y_k is the value predicted by the network, T_k is the corresponding result from the dynamic analysis and NP is the number of combinations in the database.

Thus, the mean value and the standard deviation of the response over the set of sub-combinations can be written as in Eq. (6), incorporating the relative errors from Eq. (5):

$$\begin{aligned} \overline{F}(\boldsymbol{X}) &= \overline{Y}(\boldsymbol{X})\ (1. + \sigma_{\varepsilon m}\ X_{N_1}) \\ \sigma_F(\boldsymbol{X}) &= \sigma_Y(\boldsymbol{X})\ (1. + \sigma_{\varepsilon\sigma}\ X_{N_2}) \end{aligned} \tag{6}$$

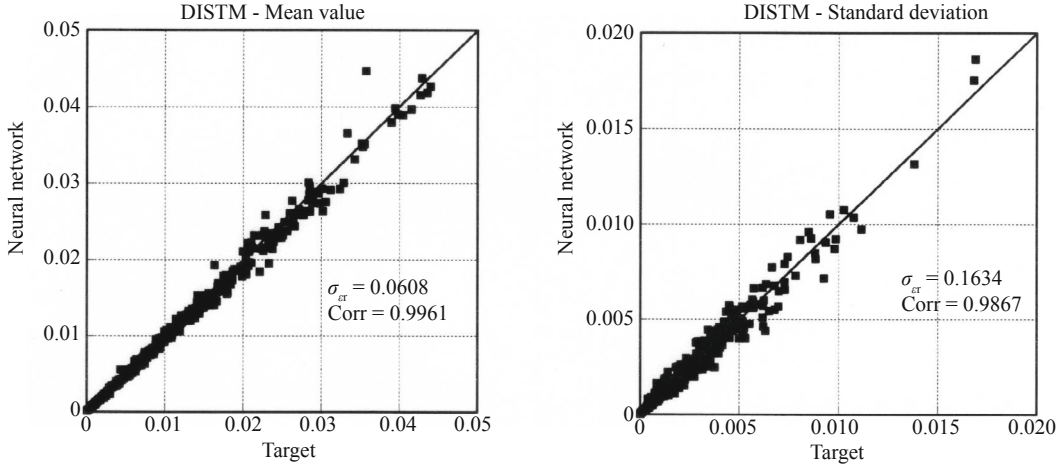

Fig. 3 Neural networks for maximum inter-story drift DISTM

in which $\overline{Y}(\boldsymbol{X}), \sigma_Y(\boldsymbol{X})$ are the mean value and standard deviations obtained from the neural networks; $\sigma_{\varepsilon m}, \sigma_{\varepsilon\sigma}$ are the deviations obtained from Eq. (5) , and X_{N1} , X_{N2} are Standard Normal random variables.

Finally, the mean values and standard deviations from Eq. (6) can be used to predict the response $R(\boldsymbol{X})$, using a Standard Normal random variable $R_{N1,}$ and assuming a Lognormal distribution to represent the variability over the sub-combinations:

$$R(\boldsymbol{X}) \cong F(\boldsymbol{X}) = \frac{\overline{F}(\boldsymbol{X})}{\sqrt{1+(\frac{\sigma_F(\boldsymbol{X})}{\overline{F}(\boldsymbol{X})})^2}} \exp\left[R_{N_1} \sqrt{\ln(1+(\frac{\sigma_F(\boldsymbol{X})}{\overline{F}(\boldsymbol{X})})^2)} \right] \quad (7)$$

Equation (7) allows a quick estimation of the responses, using the neural networks to estimate the effect of the basic variables from Table 1 and with the Standard Normal variable R_{N1} providing the variability over the sub-combinations (which include the effect of different ground motions).

5 Block 2: reliabilities

5.1 Random variables and design parameters

Table 2 shows all the random variables considered in the problem, including the basic ones shown in Table 1, and their assumed probability distribution and statistics. Each symbol "?" appearing in this table indicates a *design parameter*, that is, one of the outputs from the optimization. As shown, these are the mean values of the cross-sectional dimensions for the beams and columns, and the corresponding longitudinal reinforcement ratios.

The lognormal statistics for the peak ground acceleration a_G, $\boldsymbol{X}(10)$ in Table 2, correspond to the seismicity for the city of Mendoza, Argentina (INPRES, 1995), and are calculated as shown by Möller *et al*. (2009a), with an arrival rate n = 0.20 for earthquake magnitudes M > 5. For this city, the peak acceleration with a 10% exceedance probability in 50 years is a_G = 0.6 g.

5.2 Performance functions

Equations (8) to (15) describe the eight functions adopted to describe the structural performance at three different levels: operational, life safety and collapse. A random variable X_{N3}, Standard Normal, is introduced in order to take into account modelling error in the calculation of the demand parameters DISTM, DILOM, and DIES. It is assumed that these quantities show an uncertainty with a coefficient of variation COV = 0.10.

- Operational:

$$G_{11}(\boldsymbol{X}) = 0.005 - \text{DISTM}(\boldsymbol{X})\left[1+\text{COV}\ X_{N_3}\right] \text{ mode 1} \quad (8)$$

$$G_{12}(\boldsymbol{X}) = 0.10 - \text{DILOM}(\boldsymbol{X})\left[1+\text{COV}\ X_{N_3}\right] \text{ mode 2} \quad (9)$$

- Life Safety:

$$G_{21}(\boldsymbol{X}) = 0.015 - \text{DISTM}(\boldsymbol{X})\left[1+\text{COV}\ X_{N_3}\right] \text{ mode 3} \quad (10)$$

$$\left.\begin{aligned} G_{22}(\boldsymbol{X}) &= 0.40 - \text{DIES}(\boldsymbol{X})\left[1+\text{COV}\ X_{N_3}\right] \quad (11)\\ G_{23}(\boldsymbol{X}) &= 0.60 - \text{DILOM}(\boldsymbol{X})\left[1+\text{COV}\ X_{N_3}\right] \quad (12)\end{aligned}\right\} \text{mode 4}$$

- Collapse

$$G_{31}(\boldsymbol{X}) = 0.025 - \text{DISTM}(\boldsymbol{X})\left[1+\text{COV}\ X_{N_3}\right] \text{ mode 5} \quad (13)$$

Table 2 Random variables

Variable	$\overline{X}$	σ_x	Type	Variable	$\overline{X}$	σ_x	Type
$X(1) = m$	2.27 10^{-4}	2.27 10^{-5}	Normal	$X(10) = a_G$	94 cm/s^2	130 cm/s^2	Lognormal
$X(2) = b_b$	20 cm	1 cm	Normal	$X(11) = f_g$	2.50 Hz	0.375 Hz	Normal
$X(3) = h_b$	? cm	0.05 $\overline{X}$	Normal	$X(12) = \sigma_{\bar{a}_G}$	0	0.25	Normal
$X(4) = b_c$	30 cm	1.5 cm	Normal	$X(13) = a_G$	$X(13) = X(10)\ [1.0+X(12)]$		
$X(5) = h_c$	? cm	0.05 $\overline{X}$	Normal	$X(14) = R_{N1}$	0	1	Normal
$X(6) = \rho_s$	?	0.10 $\overline{X}$	Lognormal	$X(15) = X_{N1}$	0	1	Normal
$X(7) = \rho'_s$	?	0.10 $\overline{X}$	Lognormal	$X(16) = X_{N2}$	0	1	Normal
$X(8) = \rho_{col}$	?	0.10 $\overline{X}$	Lognormal	$X(17) = X_{N3}$	0	1	Normal
$X(9) = f_r/f'_{c0}$	0.10	0.01	Normal				

$$G_{32}(\boldsymbol{X}) = 0.80 - \mathrm{DIES}(\boldsymbol{X})\left[1 + \mathrm{COV}\ X_{N_3}\right] \quad (14)$$

$$G_{33}(\boldsymbol{X}) = 1.00 - \mathrm{DILOM}(\boldsymbol{X})\left[1 + \mathrm{COV}\ X_{N_3}\right] \quad (15)$$

mode 6

Six failure modes are considered: (1) $G_{11}(\boldsymbol{X}) \le 0$; (2) $G_{12}(\boldsymbol{X}) \le 0$; (3) $G_{21}(\boldsymbol{X}) \le 0$; (4) $G_{22}(\boldsymbol{X}) \le 0$ and $G_{23}(\boldsymbol{X}) \le 0$; (5) $G_{31}(\boldsymbol{X}) \le 0$; (6) $G_{32}(\boldsymbol{X}) \le 0$ and $G_{33}(\boldsymbol{X}) \le 0$. Two performance functions are incorporated in failure modes (4) and (6), implying that collapse is identified with failure in at least one of the two performance functions included.

The functions that have as demand the maximum inter-story drift DISTM are used to consider the failure of non-structural elements. The remaining functions are used to consider the failure of structural elements. This division is used to study separately the resulting probabilities of failure at the optimum solution.

5.5 Neural networks for reliability estimates

Within the bounds for the design parameters, and applying again experimental design, MC combinations of the design parameters $\boldsymbol{x}_d$ are selected at random. The number of combinations must be sufficiently large to cover the range in the design parameters, and the reliabilities associated with each combination are then calculated by simulation. These results are then represented by neural networks. A number MC = 180 combinations permits the training of a network with 20 neurons in one hidden layer, allowing for good accuracy in the neural network predictions.

The sample size used in the simulations for the calculation of the reliability levels was variable, as the simulations used increasingly larger samples until the coefficient of variation COV in the calculated failure probability P_f satisfied COV ≤ 0.04. In most of the cases the sample sizes required were of the order of 10^6. The computational times, however, were not excessive, given the use of the neural network representation for the nonlinear responses of the structure.

The reliability indices $b_j(\boldsymbol{x}_d)$ (j = 1, 6) calculated for each combination of design parameters are then represented by means of neural networks. The predictions from these networks are very good, as shown in Fig. 4 for $b_3(\boldsymbol{x}_d)$ and $b_6(\boldsymbol{x}_d)$. During the subsequent optimization, these networks allow a very efficient determination of the achieved reliability levels for a given set of design parameters, in order to verify the compliance of imposed minimum reliability constraints.

6 Block 3: optimization

6.1 Objective function

The objective function used here is the total cost of the structure. This cost includes: 1) $C_0(\boldsymbol{x}_d)$, the initial construction cost; 2) $C_d(\boldsymbol{x}_d)$, the cost of repairs for damage produced by earthquakes at some time during the life of the structure; and 3) $C_s(\boldsymbol{x}_d)$, the social costs associated with the occurrence of the earthquakes. Thus,

$$C(\boldsymbol{x}_d) = C_0(\boldsymbol{x}_d) + C_d(\boldsymbol{x}_d) + C_s(\boldsymbol{x}_d) \quad (16)$$

6.1.1 Initial cost

This cost is associated with:

(a) The reinforced concrete structure itself (beams and columns). In the example for this work, the unit cost used for concrete is CUH = 4500 \$/m^3. For the steel, the unit cost is CUA = 13 \$/kg. These costs reflect both currency and conditions in Argentina. Introducing the volumes of concrete (V_{beam} and V_{col}), and the weight of steel ($P_{s,beam}$ and $P_{s,col}$), all functions of the design parameters, the initial cost of the structure is

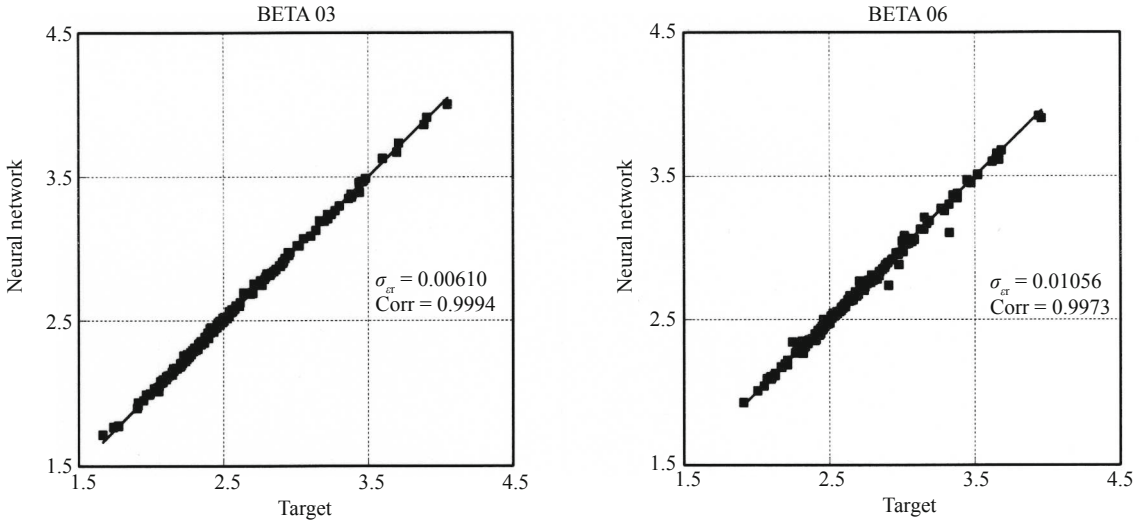

Fig. 4 Neural network approximation for reliability levels

$$C_{01}(\boldsymbol{x}_{\mathrm{d}}) = \left[V_{\mathrm{beam}}(\boldsymbol{x}_{\mathrm{d}}) + V_{\mathrm{col}}(\boldsymbol{x}_{\mathrm{d}})\right] \mathrm{CUH} + \left[P_{\mathrm{s,beam}}(\boldsymbol{x}_{\mathrm{d}}) + P_{\mathrm{s,col}}(\boldsymbol{x}_{\mathrm{d}})\right] \mathrm{CUA} \tag{17}$$

(b) Other structural elements: floor slabs and foundations. These costs are assumed deterministic and approximately estimated on the basis of the total unit cost of the building (3570 \$/m^2) and, from experience, from the relative contribution from the structure to that total unit cost (28%) and, within it, from slabs (40%) and foundations (24%). In this example, the cost associated with these other structural elements is then

$$C_{02} = 267264\,\$ \tag{18}$$

(c) Non-structural elements: these include in-fill masonry walls, floorings, doors and windows, finishings and installations, etc. From experience in Argentina, these costs amount 72% of the total building cost (the remainder 28% corresponding to the structural elements). Thus,

$$C_{03} = 1073232\,\$ \tag{19}$$

(d) Contents, including furnishings and equipment. These are estimated on the basis of the number of workstations or offices in the building, with a unit cost of 14000 \$/workstation. Assuming a total of 30 offices in the building, the cost of contents is then estimated at

$$C_{04} = 609000\,\$ \tag{20}$$

Finally, the total initial cost is obtained from

$$C_0(\boldsymbol{x}_{\mathrm{d}}) = C_{01}(\boldsymbol{x}_{\mathrm{d}}) + C_{02} + C_{03} + C_{04} \tag{21}$$

6.1.2 Repair costs

The repair costs, at present values, depend on the level of damage caused by the earthquakes, the uncertainty associated with their arrival, the number of earthquakes during the life T_{D} of the structure and the interest rate available for a repair fund from the time of construction until the occurrence of the damages.

If PR is a response used to quantify the damage to the structure, the non-structure elements and the contents, and if $C_{\mathrm{f}}(\mathrm{PR})$ is the cost of repairs required at a time t, the repair fund $C_{\mathrm{f0}}(\mathrm{PR})$ required at $t = 0$ (present value of the cost), assuming an interest rate r, is

$$C_{\mathrm{f0}}(\mathrm{PR}) = C_{\mathrm{f}}(\mathrm{PR})\ \exp(-r\,t) \tag{22}$$

Under the assumption that the structure is repaired after each event, returning it to the original conditions, the expected cost $C_{\mathrm{d}}|_{\mathrm{PR}}$ (at present values and conditional on the response PR) becomes (Möller *et al*., 2012b):

$$C_{\mathrm{d}}\big|_{\mathrm{PR}} = \sum_{n=1}^{\infty} C_{\mathrm{f}}(\mathrm{PR})\,\nu \sum_{i=0}^{n-1}\left[\frac{\nu^i}{i!}\int_0^{T_D} t^i \exp\left(-(r+\nu)t\right)\mathrm{d}t\right]\cdot \frac{(\nu T_{\mathrm{D}})^n}{n!}\exp(-\nu T_{\mathrm{D}}) \tag{23}$$

in which υ is the mean arrival rate of the earthquakes, and n is the number of earthquake events in T_{D}. In general, this cost increases with the number n, but the occurrence probability of n events in T_{D} diminishes quite rapidly with n, resulting in $C_{\mathrm{d}}|_{\mathrm{PR}}$ from Eq. (23) approaching a finite value. In this work the summation in Eq. (23) was truncated when the relative contribution of a larger n is less than 0.001. In this example the interest rate r has been assumed to be 0.05.

(a) The damage to the structure is calculated in terms of the response parameter PR = DIES, the global damage index, according to the function shown in Fig. 5. It is assumed that for DIES < 0.10 no damage needs to be repaired and that, for DIES > 0.40, the structure has sustained substantial non-repairable damage and must be completely rebuilt. The constant $a_1 = 1.20$ introduces the cost of demolition and clean-up. For damage indices less than 0.40 it is assumed that the costs reflect only the damage to beams and columns, and that no repairs are needed for floor slabs or foundations. Finally,

$$C_{\mathrm{d12}}(\boldsymbol{x}_{\mathrm{d}}) = \int_0^{\infty} C_{\mathrm{d12}}\big|_{\mathrm{DIES}} \cdot f_{\mathrm{DIES}}(\mathrm{DIES}) \cdot \mathrm{d(DIES)} \tag{24}$$

in which $f_{\mathrm{DIES}}(\mathrm{DIES})$ is the probability density function for the global damage index DIES. For a given set of design parameters $\boldsymbol{x}_{\mathrm{d}}$, and with the help of the response neural network for DIES, a Monte Carlo simulation is used to obtain the mean value and standard deviation of DIES, from which the probability density in Eq. (24) is obtained from a Lognormal distribution assumption. In Eq. (24), the index 12 implies the inclusion of costs both from Eq. (17) and those from Eq. (18), under the costs for repairs C_{f12} shown in Fig. 5.

Figure 5 assumes a linear dependency between damage index and costs, an assumption adopted here just to complete the example, but one that should be the topic of further research.

(b) The damage to the non-structural elements is calculated as a function of the maximum inter-story drift PR = DISTM, as shown in Fig. 6(a), in which the constant $a_2 = 0.30$ represents the percentage of damaged elements. Furthermore, since a total building replacement is assumed when the global damage index DIES exceeds 0.40, as shown in Fig. 6(b), the cost also includes the clean-up factor $a_3 = 1.20$. Thus, the cost for

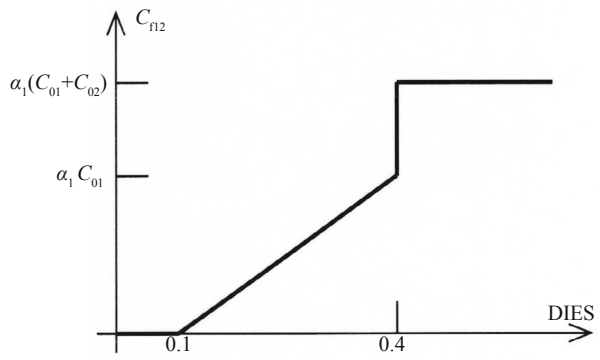

Fig. 5 Damage-cost function for the structure

repairs of non-structural elements can be expressed as

$$C_{d3}(\boldsymbol{x}_d)=\left[\int_0^{\infty} C_{d3}\big|_{DISTM}\cdot f_{DISTM}(DISTM)\cdot d(DISTM)\right]\cdot \left[1-\Pr(DIES\geq 0.4)\right]+\alpha_3\ C_{03}\ \Pr(DIES\geq 0.4) \tag{25}$$

in which f_{DISTM}(DISTM) is the probability density function for DISTM, obtained in a similar manner as that previously described for f_{DIES}(DIES).

(c) The damage to the building contents is calculated in terms of the maximum floor acceleration PR = ACELM, as shown in Fig. 7(a), in which the constant a_4 = 0.15 corresponds to an assumed percentage of damaged elements. It is also assumed that no contents can be recovered if the building totally collapses, or when the global damage index DIES exceeds 0.80, as shown in Fig. 7(b). Finally, the damage to building contents can be expressed as

$$C_{d4}(\boldsymbol{x}_d)=\left[\sum_{i=1}^{2}\int_0^{\infty} 0.5\ C_{d4}\big|_{ACELM}\cdot f_{ACELMi}(ACELM_i)\cdot d(ACELM_i)\right]\left[1-\Pr(DIES\geq 0.8)\right]+C_{04}\ \Pr(DIES\geq 0.8) \tag{26}$$

in which $f_{ACELMi}(ACELM_i)$ is the probability density function for the maximum floor acceleration $ACELM_i$, obtained in a similar way as that previously described for f_{DIES}(DIES). It is assumed that building contents are stored only in the upper two floors, and the coefficient 0.5 assumes that the contents are distributed half on the first floor and the other half on the second, with the damages estimated on the basis of the corresponding maximum floor accelerations.

Finally, the total cost for repairs is obtained from the three contributions,

$$C_d(\boldsymbol{x}_d)=C_{d12}(\boldsymbol{x}_d)+C_{d3}(\boldsymbol{x}_d)+C_{d4}(\boldsymbol{x}_d) \tag{27}$$

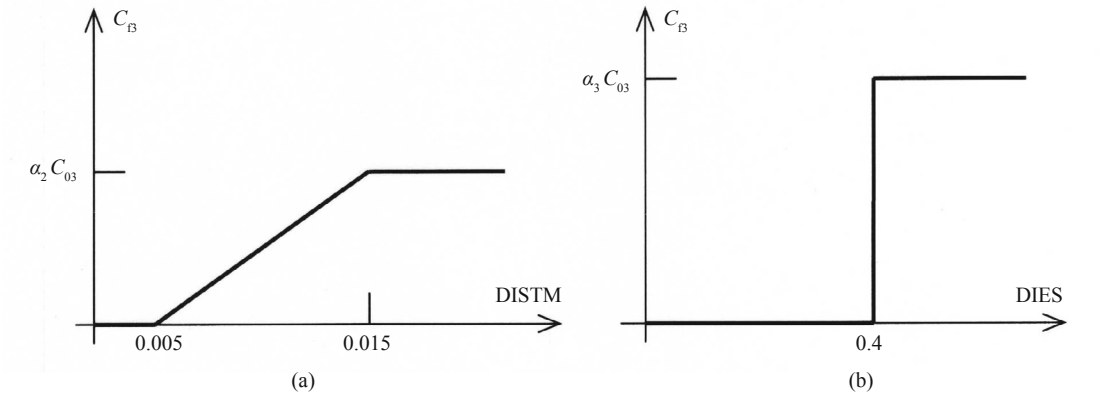

Fig. 6 Damage-cost function for the non-structural elements

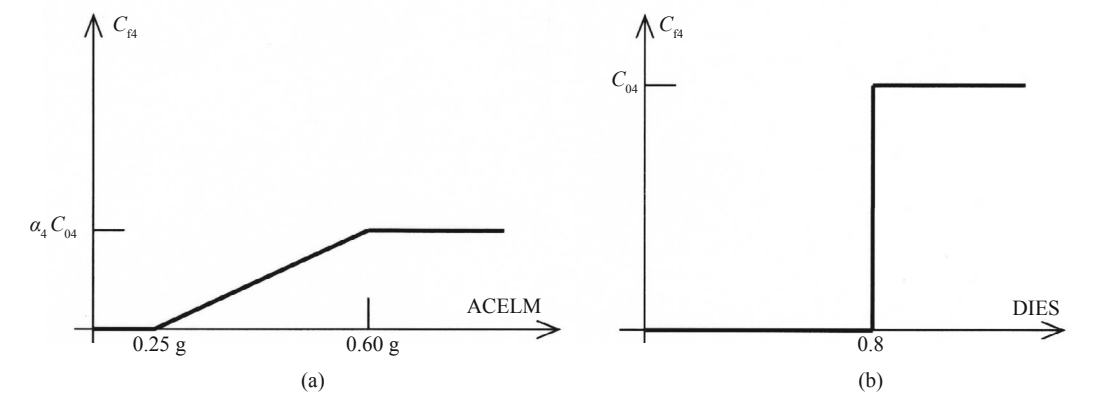

Fig. 7 Damage-cost function for building contents

It is to be noted that, even if the initial cost of non-structural elements and of the contents are not functions of the design parameters $\boldsymbol{x}_d$, their corresponding repair costs are, as these depend on the respond parameters which quantify the damage in those elements.

6.1.3 Social costs

Social costs depend on the societal context. For the example in this work, these costs are estimated in the context of Argentina. Costs that society must face, directly or indirectly, following an earthquake, could be classified as follows:

(a) Costs of re-insertion into a normal routine. Even when the earthquake produces small damage, and the population is not affected by major material or human losses, there exists a cost in helping people to psychologically adjust again to a normal routine, overcoming the fear of a recurring earthquake. These costs are associated with sessions of psychological help or counselling, here estimated as one session per week over three months. At a unit cost of \$150 per session and per person, the total cost C_{RS} is

$$C_{RS} = 54000\$ \tag{28}$$

(b) Medical and rehabilitation costs for non-fatally injured victims. On the basis of overall medical services required over three months, on an average per person of \$16710, and assuming that all 30 occupants will require medical attention, the cost C_{MR} is

$$C_{MR} = 501300\$ \tag{29}$$

(c) Costs associated with loss of life. It is, of course, more difficult to assess the economic losses due to fatalities. Here we assume only those costs that must be assumed by the owner, not by insurance companies. Labor law in Argentina requires compensation in the case of lay-off or a labor accident. At the same time, the law indicates that when the loss of life is due to an "act of God" and not from an accident, the compensation required is only 50% of the normal. Normal compensation is one month of salary for each year of service. Thus, assuming a monthly salary of \$14000 and, on average, 10 years of service, the compensation for loss of life, per person, is \$ 70000. Assuming that, in the case of a collapse, only half of the office personnel would lose their life, the total cost C_{PVH} becomes

$$C_{PVH} = 1050000\$ \tag{30}$$

(d) Costs associated with loss of business or economic activity. For the example in this work, it is assumed that the building is occupied by two companies, each with a normal monthly revenue of \$ 200000. It is also assumed that the companies can return to business after two months from the date of the earthquake. The costs associated with loss of business must also include those related to the re-acquisition of office equipment and supplies required for the busines. In this regard, a loss of \$ 30000 is added here per company. Thus, over the assumed two months of inactivity, the cost C_{LCST} is

$$C_{LCST} = 860000\$ \tag{31}$$

We have also considered the cost of rental of temporary business space during reconstruction, estimated as C_{ALQ} = \$164506. Figure 8 shows the total social cost as a function of the global damage index for the structure. Here, the costs of re-insertion for survivors of a structural collapse have been doubled.

Finally, the social costs corresponding to a set of design parameters $\boldsymbol{x}_d$ are obtained by integration using the probability density function of the global damage index DIES,

$$C_S(\boldsymbol{x}_d) = \int_0^\infty C_S\big|_{DIES} \cdot f_{DIES}(DIES) \cdot d(DIES) \tag{32}$$

since the social costs are a function of the design parameters $\boldsymbol{x}_d$ through the structural responses and the global damage index.

6.2 Reliability target constraints

Table 3 shows upper bounds for target annual failure probabilities (and associated reliability indices) according to the work by Paulay and Priestley (1992). Assuming that the arrival of earthquakes obeys a Poisson distribution, and using a mean frequency $n = 0.20$ for the city of Mendoza and magnitudes $M \geq 5$, the annual failure probability can be related to the probability of failure Pf_E if an event occurs. Thus,

$$Pf_{annual} = 1. - \exp\left[-\nu\ Pf_E\right] \ \rightarrow \ \beta_{annual} \cong -\Phi^{-1}(Pf_{annual}) \tag{33}$$

Pf_E and Pf_{annual} can be expressed in terms of the corresponding reliability indices b, providing the

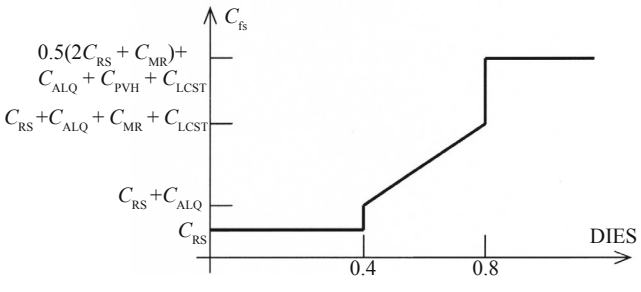

Fig. 8 Damage-social cost function

Table 3 Reliability constraints for different performance levels

Performance level	Pf_{annual}	$\beta_{j\,annual}$	Pf_E	β_{jT}
Operational	2×10^{-2}	2.054	0.10101×10^{0}	1.276
Life safety	2×10^{-3}	2.878	0.10010×10^{-1}	2.326
Collapse	$2 \times 1\ 0^{-4}$	3.540	0.10001×10^{-2}	3.090

minimum target reliability constraints for the different performance levels shown in Table 3.

$$\beta_j(\boldsymbol{x}_d) \geq \beta_{jT}, \quad j = 1, 3 \tag{34}$$

6.3 Optimization algorithm

Möller *et al*. (2012b) presented a numerical optimization search algorithm, to minimize the objective function within the bounds for the design parameters $\boldsymbol{x}_d$, while at the same time satisfying the minimum reliability constraints for the different performance levels. The following is a short description of the steps in this algorithm, which are also schematically shown in Fig. 9.

(a) The search begins from an initial or anchor point $\boldsymbol{x}_{d0,}$ which is the result of an initial design for the structure. The reliability levels corresponding to this point, $b_j(\boldsymbol{x}_{d0})$, are calculated using the reliability neural networks, and the total cost is calculated as per Section 6.1.

(b) If the preliminary design $\boldsymbol{x}_{d0}$ does not satisfy the reliability constraints from Eq. (34), then the procedure continues with steps c), d) o e). The first combination found that satisfies the constraints is then taken as the first anchor point.

(c) M1 combinations of the parameters in $\boldsymbol{x}_d$ are obtained in the proximity of $\boldsymbol{x}_{d0}$, randomly choosing a value for each of the design parameters, x_{di}, within a search zone around $\boldsymbol{x}_{d0.}$ Thus, each parameter x_{di} is modified, in turn, according to $X_{d0i} \pm$ R1 (BUD(i)-BLD (i)) , in which R1 is a constant and BUD(i) and BLD (i) are, correspondingly, the upper and lower bounds for x_{di}. The reliability constraints are verified for each of the M1 combinations. The cost is evaluated for those combinations which satisfy the constraints and, if the minimum cost among the M1 combinations is less than the cost at the anchor, the combination corresponding to that minimum is chosen as a new anchor point and the process re-started.

(d) If, among the M1 combinations, none is found to correspond to a cost lower than that for the anchor, the search is densified by choosing more combinations without exceeding a count M2.

(e) If, even after step d), no combination has been found to have a cost lower than that for the anchor, the search zone is enlarged by changing R1 to R2 = R1 + DR. The process is repeated, adding m combinations of $\boldsymbol{x}_d$ within the additional zone, with a maximum of M2. If no cost is found lower than that for the anchor, the search zone is enlarged again and the process repeated, up to a maximum of NAMP repetitions. The objective of this enlargement of the search zone is to reduce the possibility of converging to a local minimum for the cost.

(f) The process is stopped when no combination has been found with a cost lower than that for the anchor, which is then taken as the optimum combination.

The following values have been used for the example in this work: R1 = 0.15, DR = 0.05, M1 = 100, M2 = 400 and NAMP = 3.

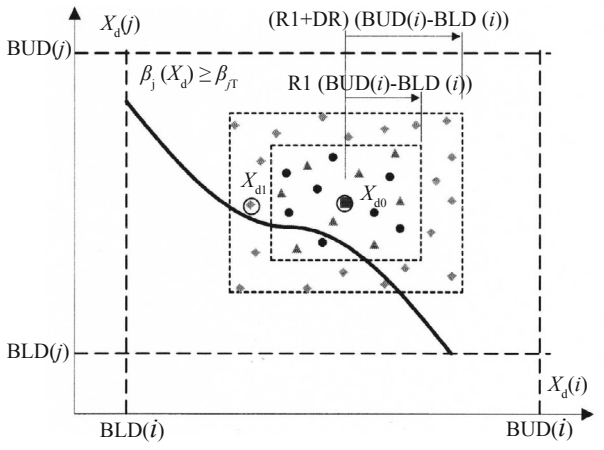

Fig. 9 Schematic representation, optimization search algorithm

7 Numerical results and discussion

The results from the optimization are shown in Table 4. These results are presented either with or without inclusion of social costs. For each of these two options, results are also shown either including or leaving out the minimum reliability constraints. For all cases, the Table also shows the reliability levels achieved, for each performance level, at the optimum design.

Under the same conditions, consideration of social costs always increases the total optimum cost. However, as shown in Table 4, individual design parameters may show a decrease when social costs are taken into account. This occurs because there are multiple combinations of design parameters that lead to almost the same total cost (Möller *et al*., 2009a). Thus, for the case without reliability constraints, Table 4 shows that the column dimension h_c reduces from 45.9 cm to 39.3 cm as social costs are introduced. This is compensated by an increase in column reinforcement ratio from 0.00856 to 0.01240.

Table 4 Optimization results

Results		Without social costs		With social costs	
		With reliability constraints	Without reliability constraints	With reliability constraints	Without reliability constraints
$x_d(1) = \overline{X}(3) = h_b$ (cm)		53.1	33.4	54.0	36.7
$x_d(2) = \overline{X}(5) = h_c$ (cm)		49.6	45.9	51.6	39.3
$x_d(3) = \overline{X}(6) = \rho_b$		0.01014	0.00798	0.00963	0.00638
$x_d(4) = \overline{X}(7) = \rho'_b$		0.01045	0.01253	0.01054	0.01243
$x_d(5) = \overline{X}(8) = \rho_c$		0.02406	0.00856	0.02173	0.01240
Performance: operational	$\beta_1(\boldsymbol{x}_d)$	1.504	1.083	1.514	1.035
	$\beta_2(\boldsymbol{x}_d)$	1.678	1.214	1.683	1.226
Performance: life safety	$\beta_3(\boldsymbol{x}_d)$	2.580	1.960	2.589	1.883
	$\beta_4(\boldsymbol{x}_d)$	2.383	1.845	2.360	1.848
Performance: collapse	$\beta_5(\boldsymbol{x}_d)$	3.095	2.415	3.096	2.268
	$\beta_6(\boldsymbol{x}_d)$	3.106	2.292	3.101	2.362
$C_{01}(\boldsymbol{x}_d)$ initial cost, structure [$]		236600	163250	238570	158090
$C_0(\boldsymbol{x}_d)$ total initial cost [$]		2186060	2112710	2188030	2107550
$C_{d12}(\boldsymbol{x}_d)$ repair costs, structure [$]		110	482	218	6174
$C_{d12}(\boldsymbol{x}_d)$ repair costs, non struc.[$]		15944	38618	14990	33886
$C_{d12}(\boldsymbol{x}_d)$ repair costs, contents [$]		33719	15930	33885	20516
$C_S(\boldsymbol{x}_d)$ social costs [$]		0	0	207960	213730
$C(\boldsymbol{x}_d)$ total cost [$]		2335900	2167800	2445100	2381900

The differences are small when minimum reliability constraints are imposed, as the performance criterion of collapse dominates the optimum solution and this criterion is associated with reduced social costs. The differences increase when the reliability constraints are lifted, to the order of 7.5%, as in this case the optimum corresponds to lower reliabilities, with increases in damage and social costs.

The reliability indices for the optimum solution are governed by the minimum reliability required for the collapse limit state, and are higher than those corresponding to the other performance levels. It can also be observed that higher reliabilities are achieved if social costs are included, clearly indicating that the optimum solution requires a lower failure probability in order to reduce the social costs.

Table 4 also presents the breakdown of costs associated with the optimum design. The differences in the initial cost $C_0(\boldsymbol{x}_d)$ is due to the contribution $C_{01}(\boldsymbol{x}_d)$ from the structure (beams and columns), as the cost $C_{02}(\boldsymbol{x}_d)$ of other structural elements, $C_{03}(\boldsymbol{x}_d)$ for non-structural elements, and $C_{04}(\boldsymbol{x}_d)$ for contents, are deterministic constants in this example and do not affect the optimum solution. The repair costs for damage to structural elements, $C_{d12}(\boldsymbol{x}_d)$, and non-structural, $C_{d3}(\boldsymbol{x}_d)$, increase when reliability constraints are not implemented, given that the resulting structure is more flexible. However, given this increased flexibility, the maximum floor accelerations are smaller and result in smaller costs for damage to contents, $C_{d4}(\boldsymbol{x}_d)$. The incidence of the social costs is of the order of 10% of the total.

Figure 10 shows the results (without minimum reliability constraints) from the evolution of the total cost objective function during the optimization process, presented in correspondence with the calculated associated annual failure probability for each performance level The minimum cost is associated with an optimum annual failure probability at each performance level and, for this example, these optima are somewhat greater than those recommended by Paulay and Priestley (1992), with the largest difference corresponding to the collapse limit state.

The lower envelope of the results in Fig. 10 (Pareto front) clearly shows that, up to a point, the total cost decreases as the annual failure probability increases. At small probabilities of failure, the total costs are controlled by the initial costs. These can be decreased if higher failure probabilities are accepted. Beyond the minimum point, increases in annual failure probability correspond to increases in costs, as a result of repair and social consequences becoming more dominant.

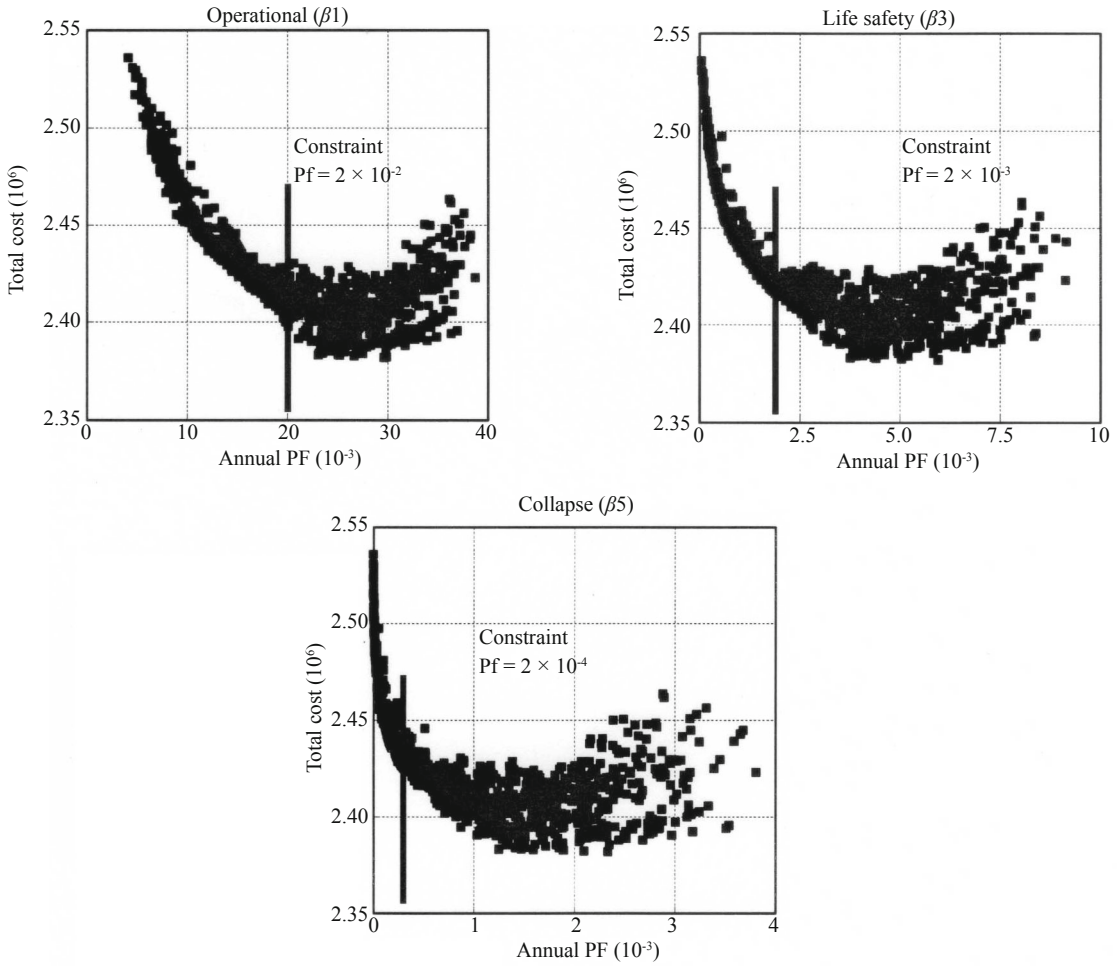

Fig. 10 Cost – Annual failure probability evolution, Pareto front and Paulay and Priestly recommendations

8 Sensitivity of the results to the magnitude of the social costs

Since the results shown here incorporate social costs only in the context of Argentina, as described in Section 6.1.3, a sensitivity analysis was performed to investigate the influence of those costs when their magnitude, from Eq. (28) through Eq. (31), were increased by a factor of 2, 3 or 5. The analyses were performed without constraints for minimum reliabilities, to emphasize the effect of the social costs. The results are shown in Table 5.

The initial structural cost, $C_{01}(\boldsymbol{x}_d)$, increases with the factor for social costs, but then slightly diminishes for a factor of 5. The same tendency is shown by the repair cost, $C_d(\boldsymbol{x}_d)$. The social costs $C_S(\boldsymbol{x}_d)$ for the optimal solutions also increase, but by factors which are somewhat less than those applied to the values from Eq. (28) through Eqs. (31).

Given that different combinations of dimensions and reinforcement ratios can result in nearly the same minimum total cost, the different cost components do not follow the same tendency among themselves when the total cost factor is increased. This is more in evidence when the incidence of social costs is greater, as these costs start to dominate the solution at minimum cost.

The incidence of the social costs in the optimal total cost increases from 9% (for the nominal case), to 15.2% (for a factor of 2), 18.4% (for a factor of 3) to 29.1% (for a factor of 5). Of course, although these results show a general tendency, specific contributions would depend on the relative weight of the different cost components.

The results in Table 5 show that the procedure outlined here permits the estimation of the influence of social costs on the achieved reliability levels at each of the required performance levels.

Table 5 Sensitivity of results to magnitude of social costs

Results		Without reliability constraints			
		Social costs factor = 1	Social costs factor = 2	Social costs factor = 3	Social costs factor = 5
$x_d(1) = \overline{X}(3) = h_b$ (cm)		36.7	45.1	65.2	54.0
$x_d(2) = \overline{X}(5) = h_c$ (cm)		39.3	41.3	34.1	40.8
$x_d(3) = \overline{X}(6) = \rho_b$		0.00638	0.00667	0.01111	0.00900
$x_d(4) = \overline{X}(7) = \rho'_b$		0.01243	0.01210	0.01069	0.01050
$x_d(5) = \overline{X}(8) = \rho_c$		0.01240	0.00918	0.00919	0.00935
Performance: operational	$\beta_1(\boldsymbol{x}_d)$	1.035	1.034	1.044	0.968
	$\beta_2(\boldsymbol{x}_d)$	1.226	1.330	1.480	1.467
Performance: life safety	$\beta_3(\boldsymbol{x}_d)$	1.883	1.882	1.760	1.858
	$\beta_4(\boldsymbol{x}_d)$	1.848	1.827	2.061	2.005
Performance: collapse	$\beta_5(\boldsymbol{x}_d)$	2.268	2.276	2.132	2.329
	$\beta_6(\boldsymbol{x}_d)$	2.362	2.285	2.550	2.468
$C_{01}(\boldsymbol{x}_d)$ initial cost, structure [$]		158090	172950	197620	189390
$C_0(\boldsymbol{x}_d)$ total initial cost [$]		2107550	2122410	2147080	2138850
$C_d(\boldsymbol{x}_d)$ repair costs [$]		60576	65270	114099	89939
$C_S(\boldsymbol{x}_d)$ social costs [$]		213730	392550	509160	918210
$C(\boldsymbol{x}_d)$ total cost [$]		2381900	2580300	2770400	3147000

9 Conclusions

This work has presented a general framework for the performance-based design optimization of a building under seismic demands, for minimum total cost with minimum reliability levels at each of three performance levels. This framework, instead of using the usual fragility approach, works directly with the set of structural and ground motion variables. This, plus neural network representation for responses and achieved reliabilities in the different limit states, permits the performance-based design optimization for the chosen design parameters like dimensions and amounts of reinforcement, at a minimum total cost.

The framework has been illustrated using the case of a three-story office building, with the seismicity corresponding to the city of Mendoza, Argentina. The optimization for minimum total cost has taken into account the initial costs of the structure, the non-structural elements and the contents, as well as a way for considering the repair costs following earthquakes during the life cycle of the building and the associated social costs.

The calculations are efficiently divided into different independent blocks: the dynamic structural responses, reliability calculations for each performance level and, finally, the optimization itself. The use of neural networks for the representation of dynamic responses makes efficient the calculation of reliabilities via simulation. Further, the use of neural networks to represent the reliability levels as functions of the design parameters, makes efficient both the optimization and the verification of whether minimum reliability constraints were being satisfied.

The numerical results obtained are coherent and show the importance of considering, in the total, not only the initial cost of the structure but also those associated with future repairs and social costs related to the earthquake event. For the example studied, the incidence of the social costs in the optimum solutions was in the order of 10% of the total. When the optimization is carried out without imposing minimum reliability constraints, the optimum probabilities of failure corresponding to the minimum cost resulted, for the example shown, in values somewhat greater than those levels recommended in the literature.

A sensitivity analysis has shown that the optimal total cost is quite dependent on the magnitude on the assumed social costs, implying that careful consideration of the latter, in relation to the other cost components, is a requirement for a realistic optimization or performance-based design of the structure. Generally, the framework presented is a useful tool to aid decisions related to total cost and risks in earthquake engineering.

References

Bertero VV (1997), "Performance-based Seismic Engineering: a Critical Review of Proposed Guidelines," *Seismic Design Methodologies for the Next Generation of Codes*, Fajfar P and Krawinkler H (Eds.), AA Balkema, Rotterdam, 1–31.

Bertero VV and Zagajeski SW (1979), "Optimal Inelastic Design of Seismic-resistant Reinforced Concrete Framed Structures," *Nonlinear Design of Concrete Structures*, CSCE-ASCE-ACI-CEB International Symposium, Ontario, Canada.

FEMA 356 (2000), "Prestandard and Commentary for the Seismic Rehabilitation of Buildings," American Society

of Civil Engineering (ASCE), Federal Emergency Management Agency, USA.

Filippou FC, D'Ambrisi A and Issa A (1992), "Nonlinear Static and Dynamic Analysis of Reinforced Concrete Subassemblages," Earthquake Engineering Research Center, *Report N° EERC 92-08*, University of California, Berkeley.

Fragiadakis M, Lagaros ND and Papadrakakis M (2006), "Performance-based Multiobjective Optimum Design of Steel Structures Considering Life-cycle Cost," *Structural and Multidisciplinary Optimization*, **32**(1): 1–11.

Gencturk B (2012), "Life-cycle Cost Assessment of RC and ECC Frames Using Structural Optimization," *Earthquake Engineering & Structural Dynamics*, **42** (1): 61–79.

Gencturk B and Elnashai AS (2012), "Life Cycle Cost Considerations in Seismic Design Optimization of Structures," *Structural Seismic Design Optimization and Earthquake Engineering: Formulations and Applications*, Plevris V (ed), IGI Global, Chapter 1: 1–22.

Ghobarah A (2001), "Performance-based Design in Earthquake Engineering: State of Development," *Engineering Structures*, **23**(8): 878–884.

Hamburger R, Rojahn C, Moehle J, Bachman R, Comartin C and Whittaker A (2004), "The ATC-58 Project: Development of Next-generation Performance-based Earthquake Engineering Design Criteria for Buildings," *Proc. 13th World Conference on Earthquake Engineering,* Vancouver, BC, Canada, Paper No. 1819.

Hurtado J (2004), *Structural Reliability – Statistical Learning Perspectives*, Lecture Notes in Applied and Computational Mechanics, **17**, Springer Verlag.

INPRES (1995) "Microzonificación Sísmica del Gran Mendoza", *Publicación Técnica N° 19*, Instituto Nacional de Prevención Sísmica, San Juan, Argentina.

INPRES-CIRSOC 103 Parte 1 (2008), "Reglamento Argentino Para Construcciones Sismorresistentes," *Instituto Nacional de Tecnología Industrial*, Argentina.

Lagaros ND and Papadrakakis M (2007), "Seismic Design of RC Structures: A Critical Assessment in the Framework of Multi-objective Optimization," *Earthquake Engineering & Structural Dynamics*, **36**(12): 1623–1639.

Liu M, Burns SA and Wen YK (2006), "Genetic Algorithm Based Construction-conscious Mínimum Weight Design of Seismic Steel Moment-resisting Frames," *Journal of Structural Engineering*, **132**(1): 50–58.

Melchers RE (1987), *Structural Reliability: Analysis and Prediction*, Ed. Ellis Horwood Limited – Halsted Press: A Division of John Wiley & Sons.

Möller O (2001), "Metodología Para Evaluación de la Probabilidad de falla de Estructuras Sismorresistentes y Calibración de códigos," *Tesis de Doctorado en Ingeniería*, Universidad Nacional de Rosario, Argentina.

Möller O, Ascheri JP, Foschi R and Rubinstein M (2012a), "Optimización Estructural para Costo Mínimo con Restricciones de Confiabilidad: Evaluación de Alternativas de Diseño Sísmico," *Mecánica Computacional*, Vol. **XXXI**: 2527–2545.

Möller O and Foschi R (2003), "Reliability Evaluation in Seismic Design: a Response Surface Methodology," *Earthquake Spectra*, **19**(3): 579–603.

Möller O, Foschi R, Quiroz L and Rubinstein M (2009a), "Structural Optimization for Performance-based Design in Earthquake Engineering: Applications of Neural Networks," *Structural Safety*, **31**(6): 490–499.

Möller O, Foschi R, Rubinstein M and Quiroz L (2006), "Momento-curvatura de Secciones de Hormigón Armado Sismorresistentes Utilizando Redes Neuronales," *Mecánica Computacional*,Vol. **XXV**: 2145–2162.

Möller O, Foschi R, Rubinstein M and Quiroz L (2009b), "Seismic Structural Reliability Using Different Nonlinear Dynamic Response Surface Approximations," *Structural Safety*, **31**(5): 432–442.

Möller O, Foschi R, Rubinstein M and Savino F (2010), "Optimización, Con Requisitos de Confiabilidad, A Partir del Diseño Preliminar de Pórticos Sismorresistentes," *Mecánica Computacional*, Vol. **XXIX**: 1403–1421.

Möller O, Foschi R, Rubinstein M and Savino F (2012b), "Performance-based Seismic Design: a Search-based Cost Optimization with Minimum Reliability Constraints," *Structural Seismic Design Optimization and Earthquake Engineering: Formulations and Applications*, Plevris V (Ed), IGI Global, Chapter 2: 23–50.

Park YJ and Ang AH-S (1985), "Mechanistic Seismic Damage Model for Reinforced Concrete," *Journal of Structural Engineering*, ASCE, **111**(ST4): 722–739.

Paulay T and Priestley MJN (1992), *Seismic Design of Reinforced Concrete and Masonry Buildings*, John Wiley & Sons, Inc.

Pérez López JR (2005), "Contribución a Los Métodos de Optimización Basados en Procesos Naturales y su Aplicación a la Medida de Antenas en Campo Próximo," *URL http://www.tesisenred.net/TDR-0305107–180847*.

Pezeshk S (1998), "Design of Framed Structures: An Integrated Non-linear Analysis and Optimal Mínimum Weight Design," *International Journal for Numerical Methods in Engineering*, **41**(3): 459–471.

SEAOC Vision 2000 Committee (1995), "Performance based Seismic Engineering of Buildings," Structural Engineers Association of California, Sacramento, California, U.S.A.

Shinozuka M and Sato Y (1967), "Simulation of Nonstationary Random Processes," *Journal of Engineering Mechanics*, ASCE, **93**(1): 11-40.

Swisher JR, Hyden PD, Jacobson SH and Schruben LW (2000), "A Survey of Simulation Optimization Techniques and Procedures," *2000 Winter Simulation Conference*, Joines JA, Barton R, Kang K and Fishwick PA (Eds).